THERMAL CONTROL SYSTEMS FOR
LOW-TEMPERATURE HEAT REJECTION
ON A LUNAR BASE

K. R. Sridhar

Principal Investigator

and

Matthias Gottmann

Graduate Research Assistant

Department of Aerospace and Mechanical Engineering

The University of Arizona

Tucson, AZ 85721

Nomenclature

T	—	temperature	L	—	rejection loop pipe length
P	—	pressure	A	—	radiator area
h	—	enthalpy	H	—	radiator equivalent height
s	—	entropy	S	—	radiator array distance to lunar base
ρ	—	density	σ_y	—	material strength
$\dot{m}$	—	mass flow rate	d	—	inner pipe diameter
$\dot{V}$	—	volumetric flow rate	l	—	pipe length
Q	—	heat load	f	—	friciton factor
q	—	specific heat load	v	—	fluid velocity
W	—	compressor power	Re	—	Reynolds number
w	—	specific compressor power	c_p	—	specific heat at constant pressure
COP	—	coefficient of performance	μ	—	dynamic viscosity
η	—	efficiency	σ	—	Stefan Boltzmann constant
m	—	specific mass	ϵ	—	emissivity
M	—	mass			

1 Introduction

One of the important issues in the lunar base architecture is the design of a Thermal Control System (TCS) to reject the low-temperature heat from the base. The TCS ensures that the base and all the components inside are maintained within the operating temperature range. The temperature of the lunar surface peaks to 400K during the 336 hour lunar day and heat rejection from the base under such conditions is a technically challenging task. Prior studies have shown that the overall mass of a TCS and its power supply for lunar base applications can be significant. The single largest fraction of the overall mission cost for any space mission is associated with the initial launch, which continues to be in the vicinity of $ 5000/lb from Earth to LEO. The reduction of lift mass at launch is a key driver in reducing the overall cost of space missions. In order to find the lowest mass for the TCS, several options have been proposed. One option would be to store the waste heat deep in lunar regolith [1]. A piping system working as a heat exchanger has to be buried in the soil. The technical difficulties and uncertainties associated with large scale excavation on the Moon, and lack of knowledge about the thermal properties of lunar regolith are primary reasons for not pursuing this path presently. A significant portion of the total mass of the TCS is due to the radiator. In order to reduce the mass of the radiator, the concept of shaded light-weight radiators have been proposed [2]. Shading the radiator from the sun and the hot lunar soil could decrease the radiator operating temperature significantly. This technology requires shades built of specular surfaces. The degradation of the radiator

3
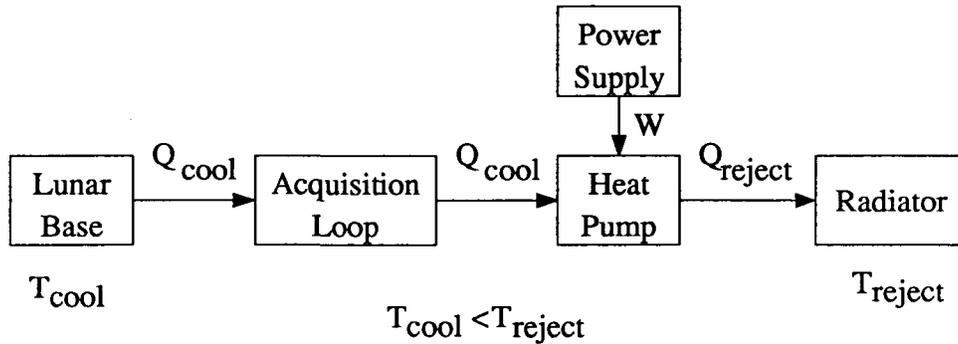
Figure 1: Schematic Diagram of a TCS using a Heat Pump

surface properties with age in a lunar environment is not known. At least for the initial

cases, the prudent approach would be to employ systems that rely on proven technology.

The concept of using a heat pump fits this bill. In this concept, energy in the form of

heat or work, is supplied to the heat pump which collects heat from the low-temperature

source (the lunar base) and delivers it at a higher temperature to the radiator. The mass

of the radiator dissipating the high temperature heat would be significantly lower than

one operating without a temperature lift. A simplified block diagram of this concept is

illustrated in figure 1.

Heat pumps have been in use for terrestrial applications for a long time. Refrigeration

devices utilizing a thermodynamic cycle are essentially heat pumps. A vapor compression

cycle involving two constant pressure and two adiabatic processes is the most widely used.

It is also called a Rankine cycle and requires shaft work. Absorption cycles on the other

hand are heat driven and do not require high quality shaft power. The Stirling cycle consists

of two isothermal and two constant volume processes and promises a better efficiency than

the Rankine cycle. Theoretically, it reaches the same efficiency as the optimal Carnot cycle but the processes are technically difficult to realize. Today, Stirling cycle coolers are used in cryogenic applications. Experiments using this cycle for residential heat pumps show promising results [3],[4], but but these heat pumps are yet to become technically reliable.

To optimize the mass of the heat pump augmented TCS, all promising options have to be evaluated and compared. During these preliminary comparison studies, considerable care is given to optimizing system operating parameters, working fluids and component masses. However, to keep this preliminary study simple and concise, the following aspects are not considered presently. The systems are modeled for full load operation and the implications and power penalties at off-design and partial load conditions are not considered. However, it is realized that the surface temperature of the lunar regolith varies considerably during the lunar day as shown in figure 2 . This variation in the regolith temperature would indicate that the temperature lift and the load of the heat pump would vary as a function of the time of the day. For this reason, the performance of the heat pump at partial load conditions is important and will be studied in detail in the future. Also, redundancy requirements are not considered presently. While evaluating system mass, the control components are not accounted for since the variation in their masses for the various cycles and working fluids would not be large. Issues such as these will be studied in detail during the design of the actual system.
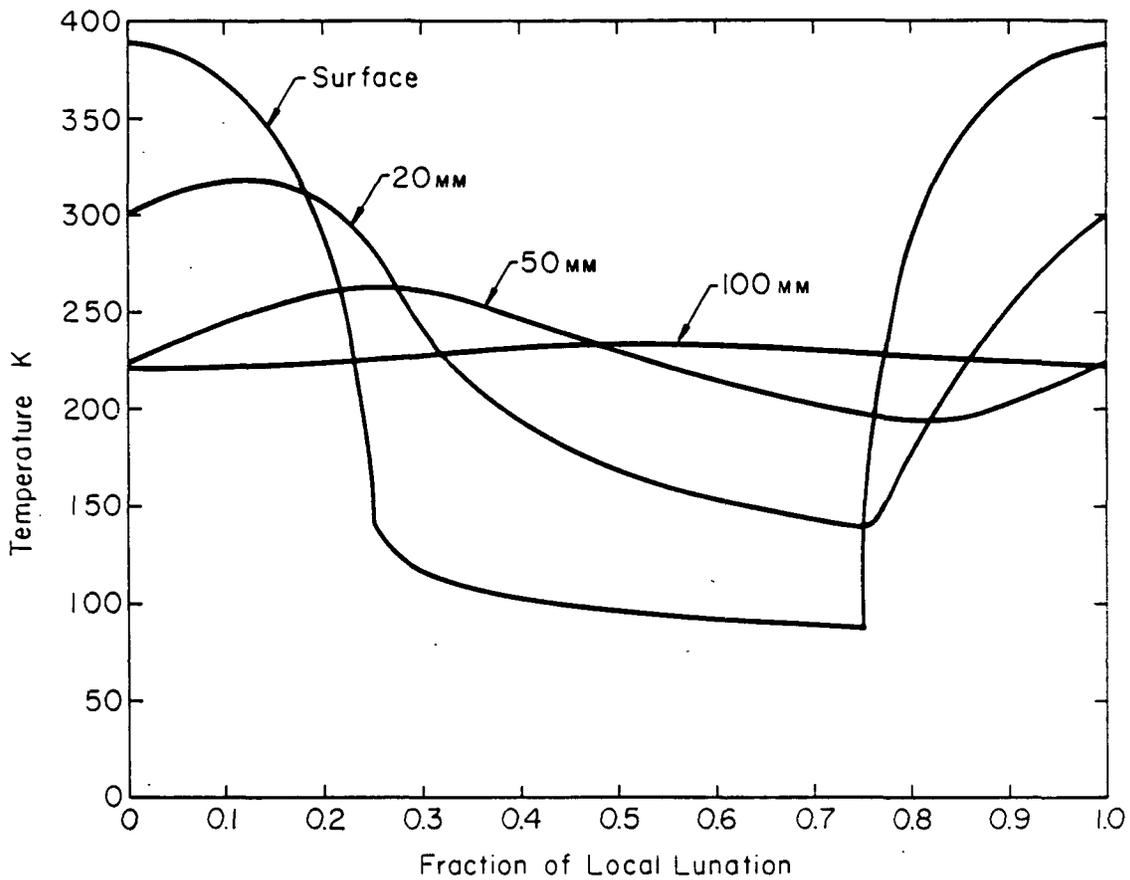
2 Rankine Cycle Heat Pump

A study was conducted to optimize a heat pump operating on a Rankine cycle. The details are presented in this and the following sections

2.1 Cooling Load

To estimate the cooling load a closed system analysis was performed on the lunar base. Energies crossing the boundaries are electrical power supply, conduction through walls, and

heat removed by the acquisition loop. Within the system, heat generation can occur due to human metabolic activity. The electrical power input for a first stage base is estimated to be between 50 and 100 kW, more likely 100kW ([1],[6], [7]). The conduction through the walls depends on the insulation. Without significant mass penalties it is possible to reduce heat gains or losses to a very small fraction of the electrical input, hence it is neglected. Based on food consumption, a crew member produces an average of about 150W. For a crew of six to eight members, the total heat generation would again be negligible, compared to the electrical input. Therefore, the cooling load (the heat removed by the acquisition loop) can be equated to the electrical input into the base. Stated differently, this implies that all electrical input will finally be dissipated as heat. The value for the cooling load is fixed at 100kW for this study. When further details about the design and activities of the base are known, these assumptions can be revisited and refined if necessary.

2.2   The Acquisition Loop

The acquisition loop collects the excess heat from the lunar base and transports it to the heat pump. The acquisition loop consists of cold plates and a network of connecting pipes. The heat is transported by a single phase fluid. Since the coolant in the acquisition loop circulates in the habitation module nontoxicity is a necessity from safety considerations. Water with certain trace additives to depress its freezing point would be a good candidate. For this study, it was decided that one cooling loop operating at a single pre-designed

temperature would be used. This temperature was chosen to be 275K (the lower of the two Space Station cooling loop temperatures). The variation in the temperature of the coolant has to be small enough to provide isothermal cooling for small variations in the load, yet large enough to keep the coolant flow rate within reasonable limits. The mass flow rate in the acquisition loop is $\dot{m} = Q_{cool}/(c_p \Delta T)$. If water with trace additives were used as the coolant and the temperature variation in the acquisition loop were taken to be 5K, the mass flow rate in the acquisition loop would be 4.8kg/s.

2.3 The Heat Pump

Two different heat pump setups were studied: In the first setup termed Case A the heat pump is directly connected to the rejection loop. In this case the condenser of the heat pump and the radiator are essentially the same device. The refrigerant circulating in the heat pump condenses and rejects heat in the radiator. An alternative setup is to decouple the heat pump and the rejection loop with a heat exchanger (Case B). Detailed analysis of the two cases and their pros and cons will be discussed in the following sections.

2.4 Heat Pump Connected Directly to the Rejection Loop (Case A)

A simplified schematic of a heat pump configuration directly connected to the rejection loop is illustrated in figure 3 The main parameters of interest in the design of a heat

8
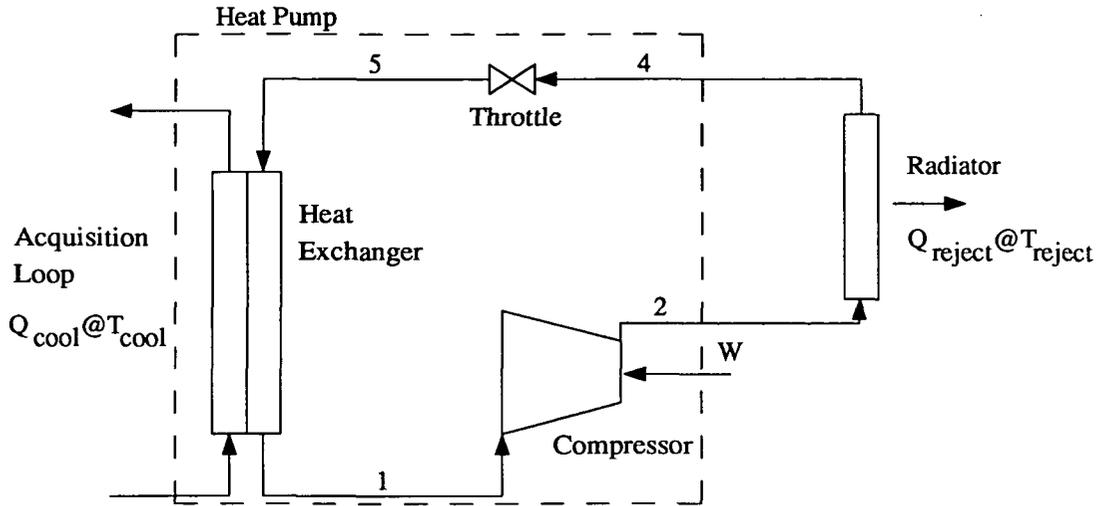
Figure 3: Schematic Diagram of a Heat Pump directly connected to the Rejection Loop

pump used for cooling are the input heat load (Q_{cool}) and its temperature (T_{low}), the

temperature lift, and the coefficient of performance (COP). The COP of a heat pump is

defined as

$$COP = \frac{Q_{cool}}{W}$$

where W is the power consumed by the heat pump.

2.4.1 The Compressor

Figure 4 illustrates the Rankine cycle process in a pressure-enthalpy diagram. The working

fluid in the vapor state is compressed from P_1 to P_2. Ideally this process would be isentropic

(2S). Due to irreversibilities, the process is nonisentropic

$$w_{ideal} = h_{2S} - h_1$$
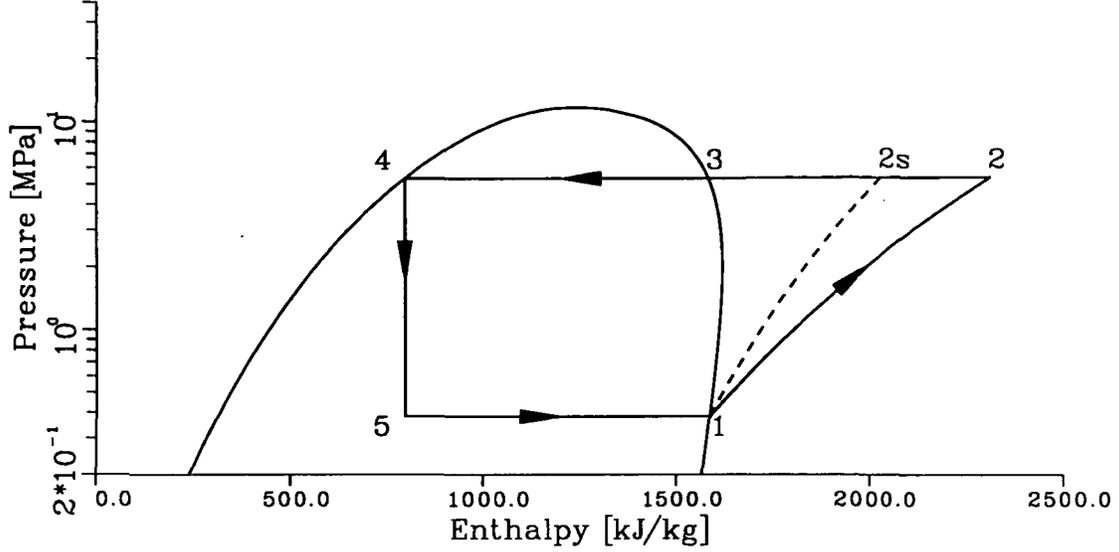
Figure 4: $P - h$ Diagram of a Rankine Cycle for R717 ($T_{low} = 270K$, $T_{high} = 360K$)

$$w_{real} = h_2 - h_1$$

$$\eta_{comp} = \frac{h_{2S} - h_1}{h_2 - h_1}$$

where: P is the pressure, h is the specific enthalpy and the subscripts refer to the states

in figure 4. It is assumed that the compression would be performed in a single stage,

in order to limit the number of free parameters. Customarily airplane cooling systems

utilize multistage compression [8], but there is no intercooling between the stages. Hence,

effectively the compression can be modeled as a single stage process. The properties of

the refrigerant used for the calculation are obtained from [9] and a FORTRAN77 code

developed in-house [10]. Deviation from the ideal behavior in the compression occur due

to mechanical, electrical (motor), and electronic (controller) inefficiencies, and fluid friction.

The values for the efficiencies in state-of-the-art aircraft cooling equipment were obtained

10

from [11], and are as follows: $\eta_{\text{mech}} = 0.95$, $\eta_{\text{electrical}} = 0.94$, $\eta_{\text{electronic}} = 0.91$, and $\eta_{\text{fluid}} = 0.75$. The overall efficiency of such a compressor would be the product of all four efficiencies, about 61 percent in this case. The excess energy supplied to overcome these inefficiencies will be converted to heat. Since the compressor would operate in a high vacuum environment, radiation to the environment and convection of the heat by the vapor flow inside are the only heat rejection mechanisms. An upper limit for the amount of heat rejected by radiation can be obtained by modeling the compressor as a black cube, 0.25m side, at 400K. Both, the surface properties and the temperature of the surface are deliberately chosen to be well above the actual values to obtain a conservative estimate . This heat is small compared to the compressor input power and can be neglected. Therefore, it can be assumed that all the energy supplied to the compressor will be used to compress and heat the refrigerant. It should be noted that the temperature of the compressor can be maintained within operating limits by the use of a cold plate. However this would not be required since the working fluid could convectively remove the excess heat from the compressor.

The next step is a mass estimate for the compressor. In aircraft cooling, the compressor mass is assumed to be proportional to the cooling load. One pound (0.454kg) per kilowatt is the value suggested [11]. Our mass optimization is performed at maximum cooling load (100kW) and this value remains unchanged in the optimization. The heat pump output temperature and hence the total heat rejected by the heat pump is varied. Since the

assumption of compressor mass being proportional to the cooling load would lead to an unrealistic constant mass estimate in our case, it was modified as follows. A proportionality was assumed between compressor mass and the heat pump output heat, which is the sum of the input heat and compressor power. The proportionality constant was arrived at as follows. The reference temperatures to obtain the proportionality factor, $T_{high} = 380K$ $T_{low} = 275K$, are values typical for an aircraft cooling system. For these temperatures and R717 as refrigerant, the heat pump overall COP is 0.805. With this value we get:

$$m_{comp} = \frac{M_{comp}}{Q_{reject}} = \frac{\left[Q_{cool}m^*_{comp}\right]}{\left[\frac{Q_{cool}(COP+1)}{COP}\right]} = 0.202\frac{kg}{kW}$$

where m_{comp} is the compressor mass in kg per kW rejected heat, M_{comp} the actual compressor mass in kg, m^*_{comp} the compressor mass in kg per kW cooling load.

2.4.2 Discharge and Return lines to and from the Radiator

At state 2 in figure 4 the refrigerant is in the superheated state. The length of the discharge line depends on the layout of the lunar base and how the radiators are spatially configured. The discharge line has to connect all the radiators to the compressor. Assuming the radiators are of constant height, it is reasonable to take the pipe length to be proportional to the radiator area, i.e. $L = S + A/H$, where L is the length that will be used to determine the pressure drop, A the radiator area, H is an "equivalent height" of the radiator, and S is the distance from the lunar base to the radiator array. Figure 5 depicts schematically

12
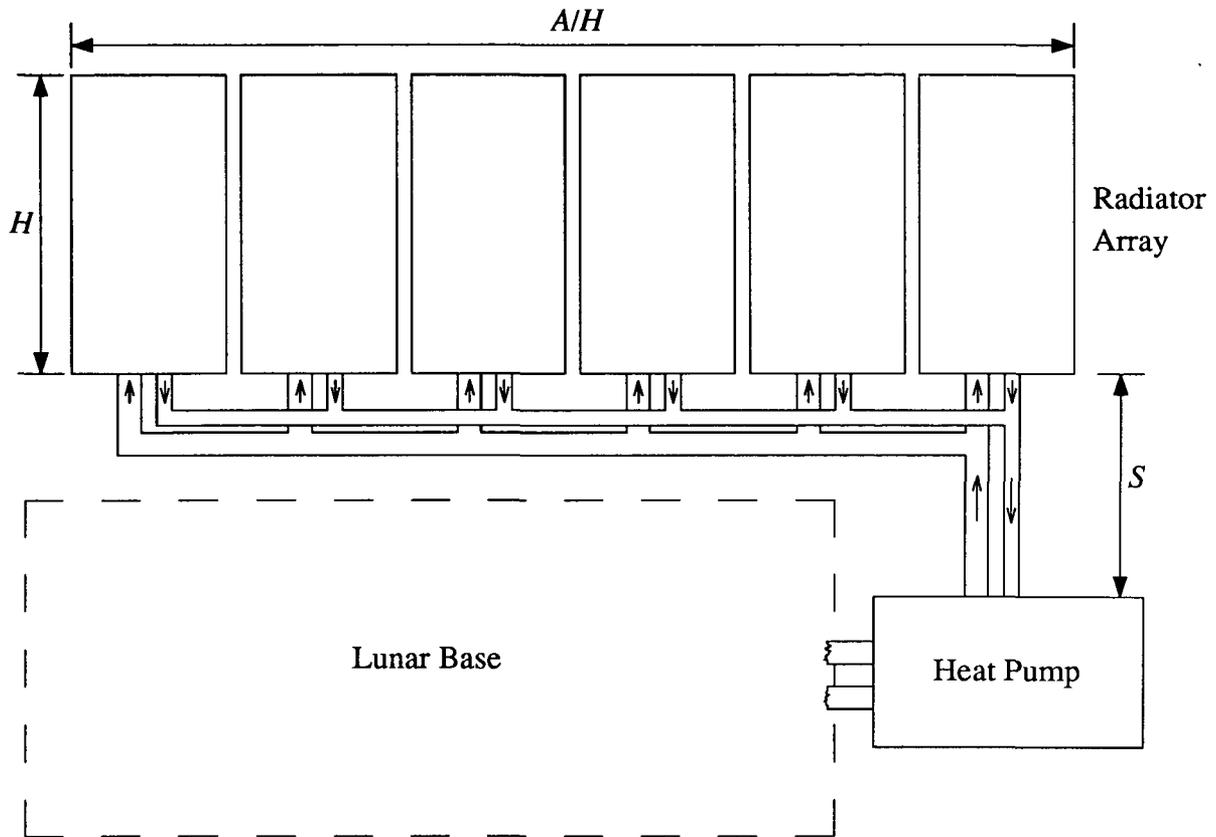
Figure 5: Schematic of Radiators and Rejection Loop Piping

the setup of the radiators and the piping. The term "equivalent height" is used because

this dimension can differ from the actual height to accommodate bends in the piping or a

spacing in between the radiators. The pipe length was defined as the distance from the heat

pump to all radiators. The complete rejection loop is $2L$. The pressure drop in the piping is

a function of the pipe diameter, and is determined based on handbook recommendations for

good design practice [12]. The pressure drop in the discharge line, the radiator (condenser)

and the return line is taken to be the equivalent of a 1K temperature drop. It is important

for the thermodynamic model that this pressure drop be small enough in order for it to not

affect the overall efficiency. The fixing of the total pressure drop also allows the designer to decouple the pipe sizing from the thermodynamic evaluation of the heat pump. The pressure drop is split such that one half of it occurs in the condenser and the rest is in the discharge and return lines. The friction losses in discharge and return lines are determined based on the optimization of the pipe masses. The frictional pressure drop, $(\Delta P)_f = \frac{f l v^2}{2 \rho d}$, where the friction factor for smooth pipes $f = \left[2 \log_{10}\left(\frac{2.51}{Re\sqrt{f}}\right)\right]^{-2}$, d is the pipe diameter, l is the length of the pipe, v the fluid velocity, ρ the fluid density, and Re the pipe Reynolds number. The total mass is the sum of the mass of the pipe and the mass of the fluid in the pipe. The tube thickness is computed based on a factor of safety of three. A minimum thickness of 0.5mm is also required. The density of the piping material is based on a light weight, high strength aluminum alloy. Should such an alloy be chemically incompatible with the refrigerant of choice, the inside of the pipes can be surface coated to take care of the problem. The masses are:

$$M_{\text{pipe}} = \frac{\pi d^2 l \rho_{\text{pipe}} P}{2 \sigma_{\text{y,pipe}}}$$

$$M_{\text{fluid}} = \frac{\pi d^2 l \rho_{\text{fluid}}}{4}$$

where $\sigma_{\text{y,pipe}}$ is the allowable (design) stress for the pipe material.

Between states 2 and 3 the superheated vapor is cooled in the radiator. Ideally this process can be modeled as an isobaric process, but due to pipe friction a small pressure

drop would occur. Between states 3 and 4, the refrigerant is condensed to saturated liquid. A finite pressure drop occurs in the condenser. The mass estimate for the condenser will be discussed in the radiator section. The heat to be rejected by the radiator, $q_{\text{reject}} = h_2 - h_4$. From state 4 the saturated liquid is sent from the radiator to the throttle valve located at the evaporator inlet, through the return line. The sizing of the return line is based on the same guidelines described for the discharge line.

2.4.3   Evaporator and Throttle Valve

Between states 4 and 5 the fluid is adiabatically throttled. The mass of the throttle valve is negligible compared to the mass of the other components of the heat pump. Between states 5 and 1, the refrigerant absorbs heat from the primary coolant circulating in the lunar base. The temperature difference between the primary coolant in the acquisition loop and the boiling refrigerant in the evaporator is 5K. The heat removed, $q_{\text{cool}} = h_1 - h_5$. The mass of the evaporator is obtained based on a suggested value of 2.72kg/kW [1].

2.4.4   Refrigerant

One of the important issues is the choice of refrigerant as the working medium for the Rankine cycle. The refrigerants that are commonly used in terrestrial and aerospace applications, R11, R12, R113, R114, and R717, were considered [8]. R113 and R114 were eliminated from the list of potential refrigerants due to the possibility of condensation of
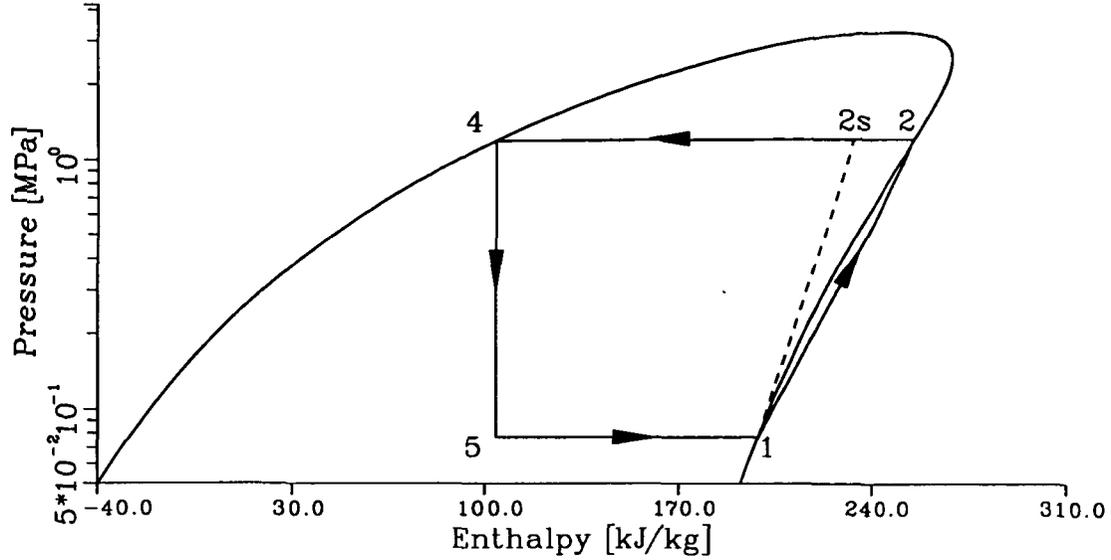
Figure 6: Rankine Cycle for R114. $T_{low} = 270K$, $T_{high} = 360K$

the vapor in the compressor (figure 6). Such condensation would be detrimental to the life

of the compressor. Among the remaining refrigerants, the selection was narrowed down

to R11 and R717, because R12 has a lower COP and a lower critical temperature (R717:

$T_{crit} = 407K$, R11: $T_{crit} = 474K$, R12: $T_{crit} = 385K$). The $P - h$ diagrams for R717 and

R11 are shown in figures 4 and 7 respectively. Safety considerations give an edge to R11

due to its nontoxicity and noninflamability, but R717 offers lower overall system mass. The

thermodynamic properties of the refrigerants were obtained using the analytical functions

suggested in [9]. The COP can be expressed in terms of the specific enthalpies and for the

Rankine cycle:

$$COP = \frac{h_2 - h_5}{h_2 - h_1}$$

16
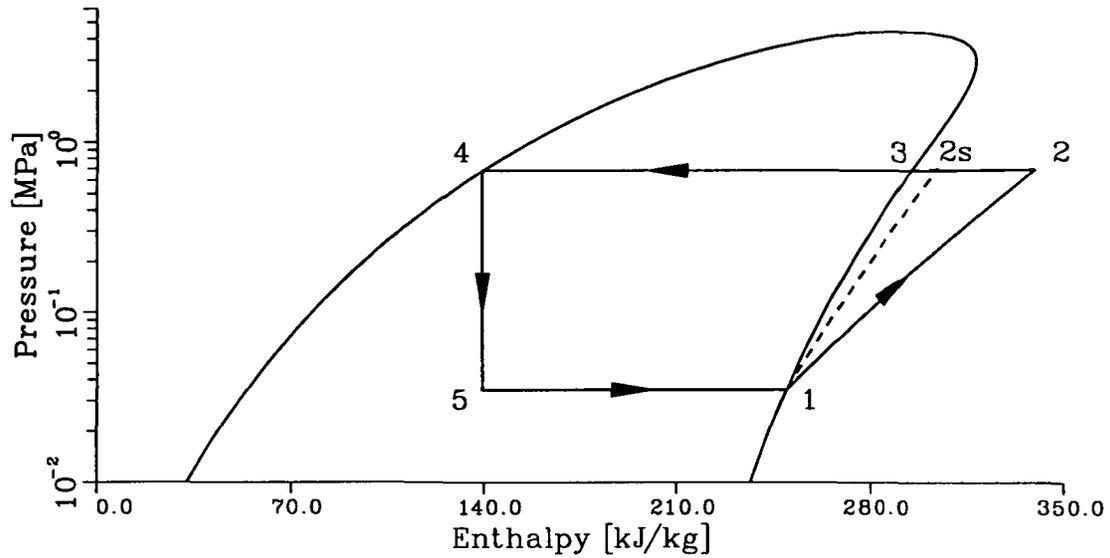
Figure 7: Rankine Cycle for R11. T_{low} = 270K, T_{high} = 360K

Table 1 illustrates the *COP* calculation for a condenser temperature of T_{high} = 380K. The overall *COP* was computed as a function of the condenser temperature and is plotted in figure 8.

2.4.5 Implementation of Heat Pump and Piping Model

Values for *COP* and the mass of the piping were computed and tabulated for varying rejection temperature using the models presented above. These tabulated values were imported into the spreadsheet and linearly interpolated where necessary.

17

Refrigerant: R717

state	T [K]	P [MPa]	h [kJ/kg]	s [kJ/kg]	ρ [kg/m^3]
1	270	0.381	1584	6.046	3.088
2	626	7.27	2419	6.615	24.89
3	380	7.14	1541	4.788	67.2
4	380	7.14	893	3.080	436.5
5	270	0.381	893	3.483	6.725
$COP = 0.829$					

Refrigerant: R11

state	T [K]	P [MPa]	h [kJ/kg]	s [kJ/kg]	ρ [kg/m^3]
1	270	0.035	249	0.9581	2.18
2	448	0.964	350	1.051	39.2
3	380	0.945	301	0.9343	49.7
4	380	0.945	158	0.5565	1255
5	270	0.035	158	0.6180	4.22
$COP = 0.914$					

Table 1: Properties in the Refrigeration Cycle for $T_{\text{high}} = 380K$

2.5 Heat Pump Decoupled from the Rejection Loop with a Heat Exchanger (Case B)

Connecting the heat pump directly to the radiator has inherent disadvantages. If the refrigerant used in the Rankine cycle is not suitable for a heat transport loop, it can be advantageous to separate the rejection loop from the heat pump with a heat exchanger. This configuration of a heat pump augmented TCS is shown in figure 9. From a system design perspective it is desirable to decouple subsystems that carry out different tasks. The decoupled case would provide for better and simpler control of the TCS during partial

18
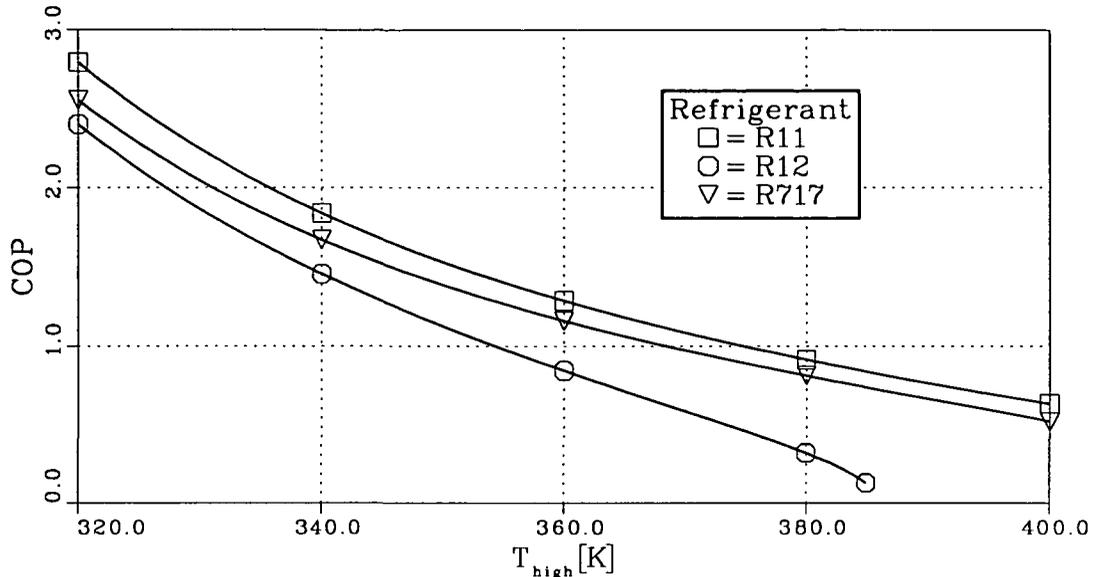
Figure 8: Variation of COP with T_{high} = 270K of R11, R12, and R717. T_{low} = 270K
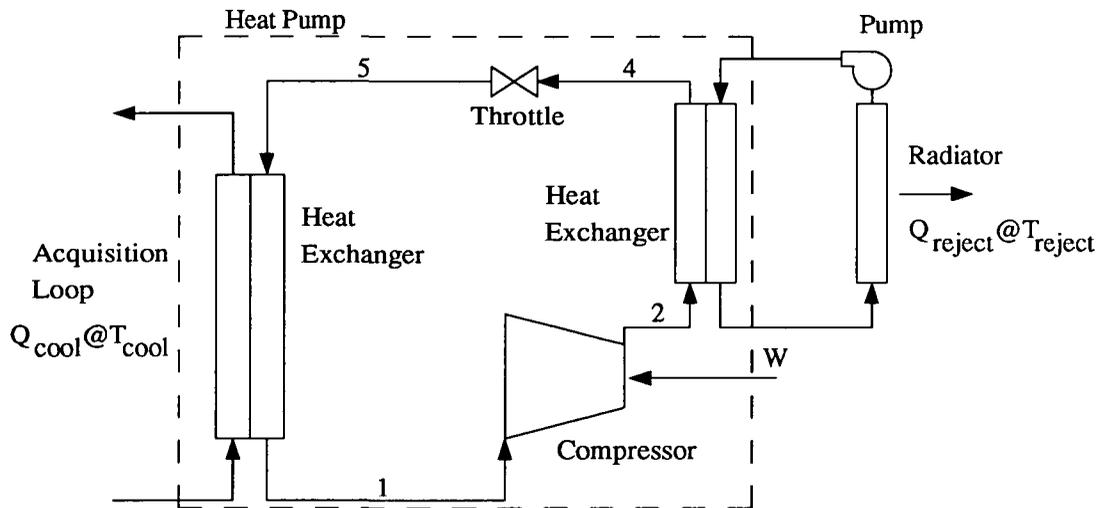
Figure 9: Schematic Diagram of a Heat Pump decoupled from the Rejection Loop

load conditions. On the other hand, a heat exchanger between the two loops will cause a temperature drop between the heat pump and the rejection loop and an associated mass penalty. To compensate for the temperature drop the heat pump has to deliver the output heat at a higher temperature and therefore operate at a lower COP. If the same fluid were

used in the Rankine cycle and in the rejection loop, the only foreseeable advantage of the decoupled system would be the possibility of better and simpler control. However, other advantages could emerge if two different fluids were used.

The thermodynamic and mass models for the heat pump with an output heat exchanger (Case B) differs only in few aspects from the models presented for Case A (section 2.4). Only these differences will be discussed in this section.

2.5.1 Condenser

In case B the condenser is a heat exchanger that decouples the rejection loop from the heat pump. Both fluids undergo phase change in this heat exchanger. For a mass estimate the value quoted in [1], 2.72 kg/kW was used. The thermodynamic performance of the condenser is characterized by a pressure drop in each loop (heat pump and rejection loop) and a temperature difference between both sides. Similar to the acquisition side, the temperature difference is set to 5K. Consistent with case A, the pressure drop has to be small enough, not to affect the heat pump performance. A pressure drop equivalent to 1K temperature drop has been assigned to the condenser.

2.5.2 Rankine Cycle Analysis

The cycle evaluation follows the same path outlined for Case A. The efficiencies and pressure drops of the heat pump components are also the same as in Case A. The *COP* as a
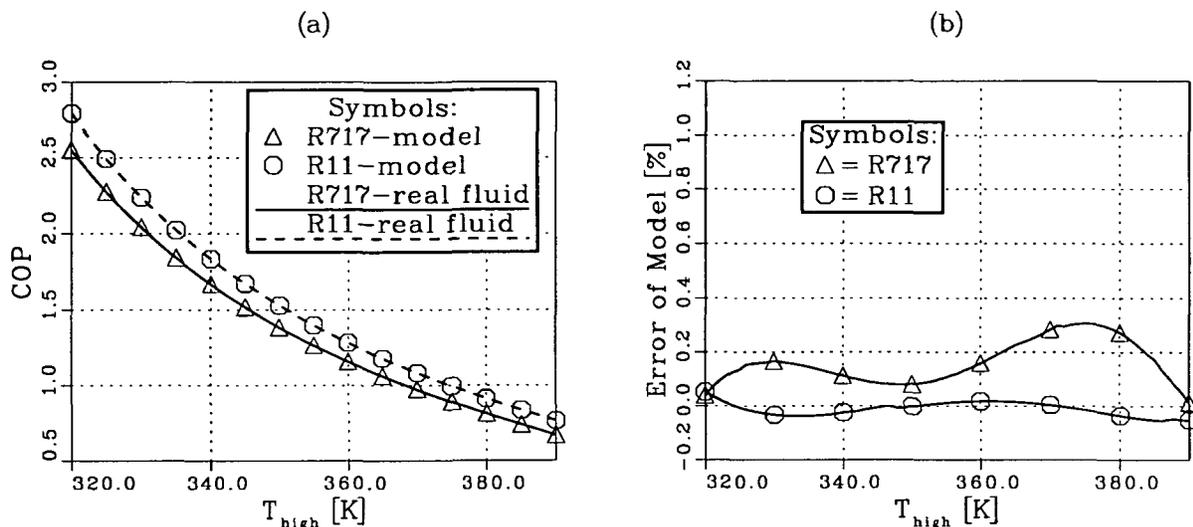
Figure 10: Comparison of COP from Cycle Analysis and Approximation for R11 and R717. $T_{\text{evaporator}} = 270K$

function of the output temperature T_{high} was computed with a FORTRAN77 program using real fluid properties from [9]. The implementation of this $COP(T)$ into the spreadsheet was realized with an approximate analytical function. For each refrigerant a fourth order polynomial was fitted to the data computed with the FORTRAN77 code. The resulting approximation yields an error of less then 0.3 percent for output temperatures from $T_{\text{high}} = 320K$ to $T_{\text{high}} = 390K$. Figures 10a and 10b show a comparison between the real fluid model and the polynomial approximation. It can be seen that the results are almost identical.

2.5.3 Rejection Loop

The decoupled rejection loop would require a pump to circulate the coolant fluid. This pump and the power penalty associated with it have to be incorporated in the mass estimate

21

and optimization. The pump mass is estimated using a formula quoted by Dexter and Haskin [13]

$$M_{\text{pump}} = 5.61 \left(\frac{\dot{m}}{60\rho} \right)^{0.75}$$

where: $\dot{m}$ is the mass flow rate in lb/hr, ρ is the density of the fluid in lb/ft^3. The power required for a liquid pump can be readily computed from

$$W_{\text{pump}} = \frac{\Delta P \dot{V}}{\eta_{\text{pump}}}$$

where ΔP is the pressure differential across the pump, $\dot{V}$ the volume flow rate, and η_{pump} the pump efficiency. A conservative $\eta_{\text{pump}} = 0.25$ as suggested by [13] was used. The pressure drop was determined with the formulas presented for case A. The pipe thickness is again determined based on the hoop stress or 0.5mm, whichever is larger. Masses included in the estimate are due to pipes, coolant, pump, and the power supply. The decoupled rejection loop does not affect the heat pump COP. The minimum mass for the loop may be achieved by balancing pipe mass and the power penalty. This approach results in optimum mass when the pipe diameters are relatively small and the pressure drop is large. However, a large pressure drop in the vapor line would result in a large temperature drop and this is accompanied by an increase in the radiator area and mass. While the pressure drop in the liquid line can be compensated with the pump, if the pressure drop gets large, the pumping power will become significant and add to the total heat rejection load.. Therefore, the mass

estimate for the piping has to be computed based on a limited pressure drop. Here again, the pressure drop is specified in terms of an equivalent temperature drop and is set to 0.5K in the vapor and 1.0K in the liquid line. These values are chosen based on recommended design practice [12]. The cooling fluid of choice is ammonia, which already demonstrated its good performance as a heat transport fluid in Case A. The toxicity of ammonia will not be a concern for the rejection loop as it is outside the habitation modules.

In Case A the piping mass was determined together with the heat pump estimate because they are coupled. Assuming values for the radiator height and distance from the base, Case A yielded a model where the piping mass depends solely on the rejection temperature. For Case B a model that makes use of the decoupling of heat pump characteristics and the rejection loop was sought. For a given refrigerant and specified pressure drops in the liquid and vapor lines, the rejection loop mass depends on three parameters: rejection heat load Q_{reject}, rejection temperature T_{reject}, and pipe length L. Using the thermodynamic properties from [9] the mass model was implemented into a FORTRAN77 code. Figures 11 and 12 show results obtained with the code. For use with a spreadsheet software it is desirable to obtain an analytical expression for the mass. This was realized with a polynomial which is second order in temperature, second order in length and linear in rejection heat load:

$$M_{\text{piping}} = \sum_{i=0}^{2} \sum_{j=0}^{2} \sum_{k=0}^{1} a_{ijk} T^i L^j Q^k$$

The coefficients were determined with a least square error fit. The approximation is valid
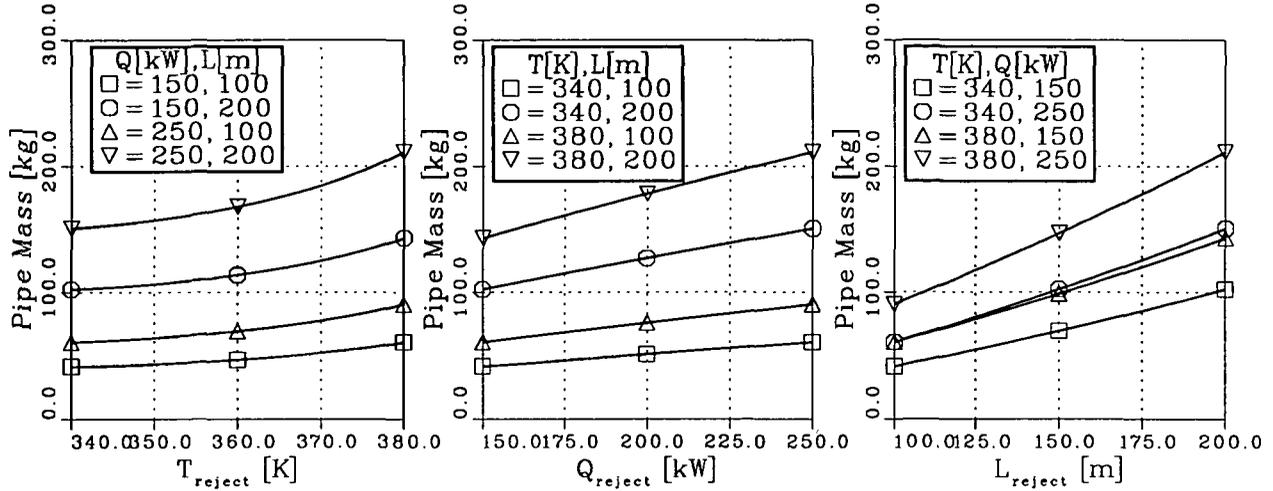
Figure 11: Mass of the Liquid Piping

in the following range: $340K \leq T_{\text{reject}} \leq 380K$, $150kW \leq Q_{\text{reject}} \leq 250kW$, and $100m \leq L \leq 400m$. The maximum error of the approximation is three percent.

2.6 Radiator Considerations

The function of the radiator is to reject the waste heat from the base. The heat rejected by the radiator is given by $Q = A\epsilon\eta\sigma(T^4_{\text{reject}} - T^4_{\text{sink}})$ where ϵ is the emissivity, η the fin efficiency, T_{reject} and T_{sink} the radiator and sink temperatures. The estimated sink temperature for a vertically mounted radiator at the lunar base is 321K [6]. Most reviewed sources suggest $\epsilon = 0.8$, and $\eta = 0.7$. Several estimates for the mass of a radiator are available in the literature ([1],[6],[14],[15]). The mass of a radiator is taken to be proportional to its area and recent publications recommend a value of $5kg/m^2$ for a one sided radiator. The vertical radiator is two sided and hence a mass estimate of $2.5kg/m^2$ is assumed. The

24
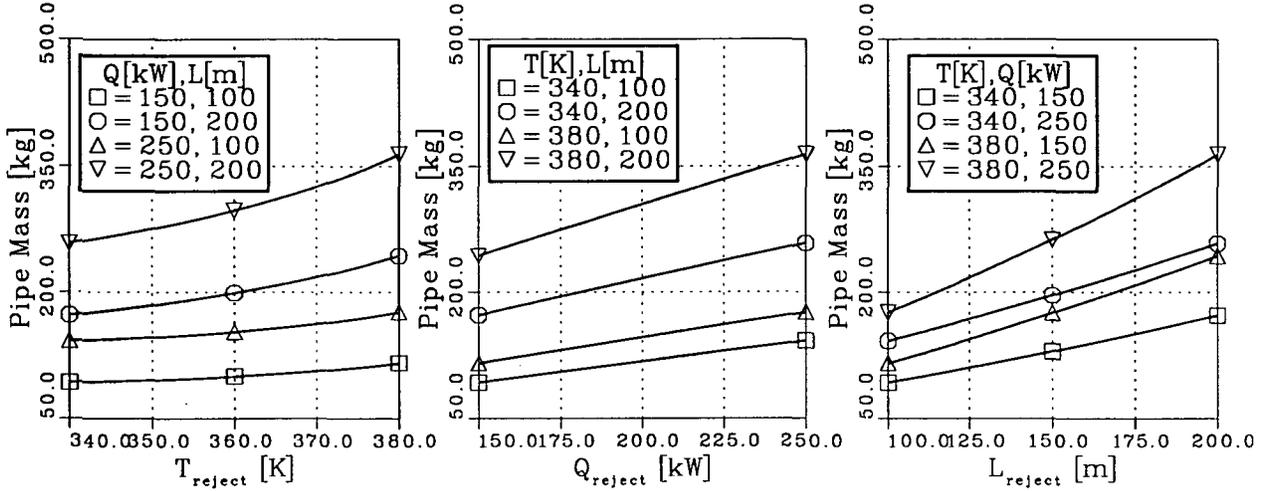
Figure 12: Mass of the Vapor Piping

heat to be rejected is the cooling load of the base plus the power consumed to operate the heat pump.

2.7 Power Supply

The heat pump consumes power to achieve the desired temperature lift. The capacity of the lunar base power station needs to be greater than otherwise, to account for this additional power consumption. It is reasonable to assume that the additional mass penalty would be proportional to the power supplied to the heat pump. A review of the literature shows that there is no consensus on the mass penalty ([1],[6],[16],[17]). The values quoted lately are in the neighborhood of 30kg/kW for nuclear units of the SP100 class [15]. This value will be used in our studies.

3 Results

The overall mass optimization was performed in a spreadsheet. The heat pump output temperature lift and hence the radiator temperature was varied and the variation of the masses of the components and the TCS were computed using the mass models described here. For the coupled TCS configuration, Case A, the analysis were performed for two working fluids, R11 and R717 and the overall TCS mass variation as a function of radiator temperature is shown in figure 13a. Similar analysis were performed for a the decoupled configuration, Case B, and the results are shown in figure 13b. For Case B, R11 and R717 were used as working fluids for the heat pump, but R717 was used in the rejection loop due to to its superior heat transport characteristics.

When R11 is used as the working fluid for the heat pump, the optimal TCS mass is 6108kg at a radiator temperature of 371K for the coupled situation, Case A. For Case B, the optimal TCS mass is 5940kg at a radiator temperature of 362K. The radiator mass in Case B is higher than for Case A due to its lower operating temperature. Also, the presence of the heat exchanger between the heat pump and the rejection loop adds extra mass to the Case B scenario. In spite of these mass penalties the optimal TCS system mass for Case B is lower than that for Case A. This is due to the huge reduction in the rejection loop piping mass for Case B. When R717 is used as the working fluid in the heat pump, the optimal mass of the TCS is 5515kg at a radiator temperature of 362K for Case A. For Case B the corresponding values are 6392kg and 360K respectively. It is obvious

that Case B is more massive than Case A since the radiator temperature for Case B is lower and also it has an additional heat exchanger.

The mass of the individual components for Cases A and B are shown graphically in figures 14 and 15 for a range of radiator temperatures and is listed in tables 2–5 for the optimal radiator temperatures.

Among the cases considered R717 coupled TCS configuration offers the least mass of 5515kg. The best decoupled configuration would involve R11 as the working fluid for the heat pump and R717 as the working fluid for the rejection loop. The optimal mass for this configuration, as stated earlier, is 5940kg. In spite of the additional mass, the decoupled system may offer the advantage of simpler and more reliable system control during partial load operation. This issue will be examined in detail in the future.
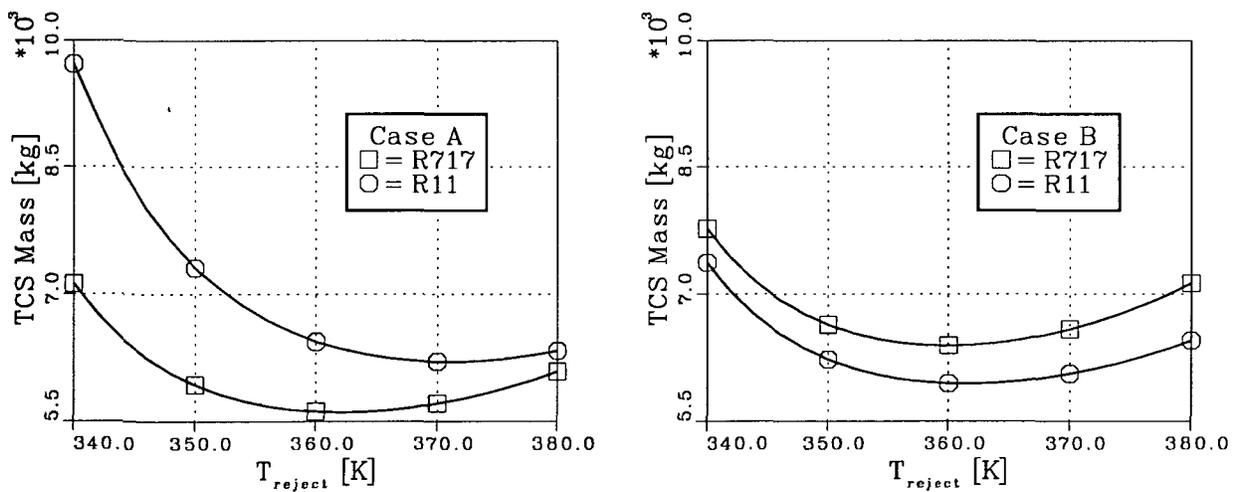

Figure 13: Overall TCS Mass as a Function of T_{reject}
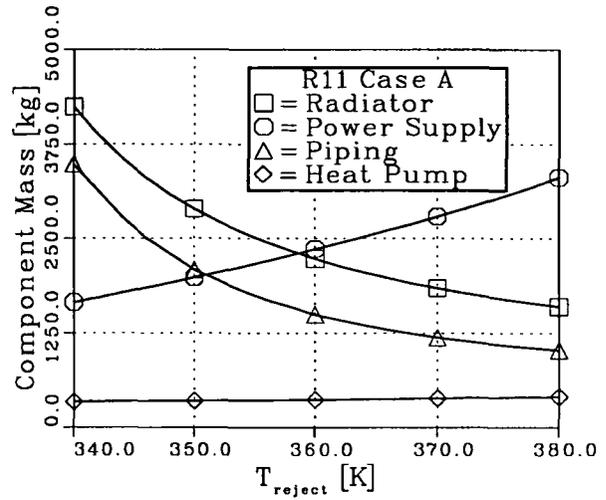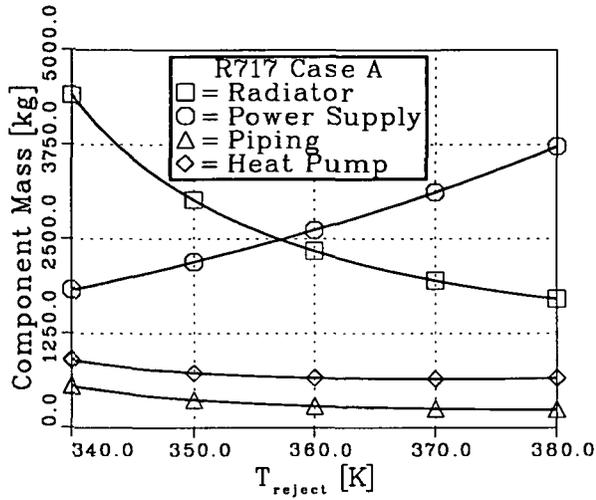
Figure 14: Component Masses as a Function of T_{reject} for Case A
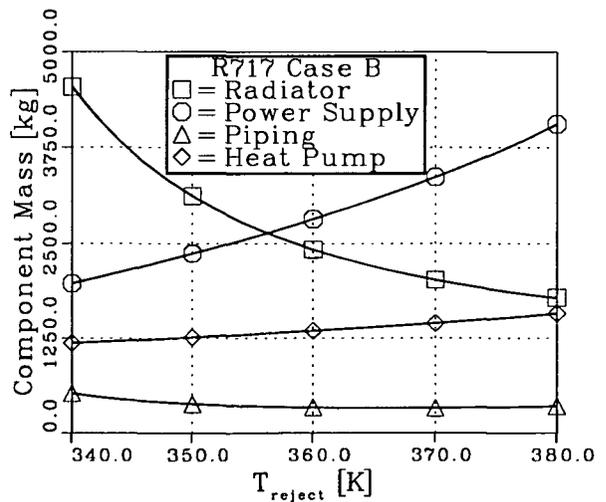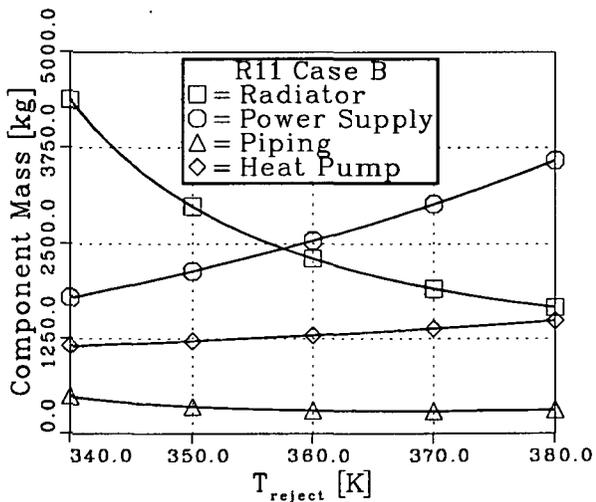
Figure 15: Component Masses as a Function of T_{reject} for Case B

28

ACQUISITION LOOP			
Cooling Load	Q_{cool}	100	kW
Cooling Temperature	T_{cool}	275	K

HEAT PUMP			
Temperature Drop HX$_{in}$	ΔT_{HXin}	5	K
Input Temperature	T_{low}	270	K
Output Temperature	T_{high}	362	K
Heat Pump Efficiency	COP	1.11	
Compressor Power	W	90.2	kW
Rejection Heat Load	Q_{reject}	190.2	kW
Evaporator Spec. Mass	m_{evap}	2.72	kg/kW
Compressor Spec. Mass	m_{comp}	0.202	kg/kW
Evaporator Mass	M_{evap}	272	kg
Compressor Mass	M_{comp}	18.2	kg
Heat Pump Mass	M_{HP}	290.2	kg

POWER SUPPLY			
Power Supply Spec. Mass	m_{power}	30	kg/kW
Power Penalty	M_{power}	2707	kg

REJECTION LOOP			
Pipe Mass	M_{pipe}	278.2	kg

RADIATOR			
Rejection Temperature	T_{reject}	362	K
Sink Temperature	T_{sink}	320	K
Fin Efficiency	η	0.7	
Emissivity	ϵ	0.8	
Radiator Area	A	895.9	m^2
Radiator Spec. Mass	m_{rad}	2.5	kg/m^2
Radiator Mass	M_{rad}	2239.8	kg

SYSTEM			
System Mass	M_{TCS}	5515	kg

Table 2: Optimum Component and TCS Mass for Case A with R717

ACQUISITION LOOP			
Cooling Load	Q_{cool}	100	kW
Cooling Temperature	T_{cool}	275	K

HEAT PUMP			
Temperature Drop HX$_{in}$	ΔT_{HXin}	5	K
Input Temperature	T_{low}	270	K
Output Temperature	T_{high}	371	K
Heat Pump Efficiency	COP	1.06	
Compressor Power	W	94.5	kW
Rejection Heat Load	Q_{reject}	194.5	kW
Evaporator Spec. Mass	m_{evap}	2.72	kg/kW
Compressor Spec. Mass	m_{comp}	0.202	kg/kW
Evaporator Mass	M_{evap}	272	kg
Compressor Mass	M_{comp}	19.1	kg
Heat Pump Mass	M_{HP}	291.1	kg

POWER SUPPLY			
Power Supply Spec. Mass	m_{power}	30	kg/kW
Power Penalty	M_{power}	2836	kg

REJECTION LOOP			
Pipe Mass	M_{pipe}	1170.5	kg

RADIATOR			
Rejection Temperature	T_{reject}	371	K
Sink Temperature	T_{sink}	320	K
Fin Efficiency	η	0.7	
Emissivity	ϵ	0.8	
Radiator Area	A	724.2	m^2
Radiator Spec. Mass	m_{rad}	2.5	kg/m^2
Radiator Mass	M_{rad}	1810.5	kg

SYSTEM			
System Mass	M_{TCS}	6108	kg

Table 3: Optimum Component and TCS Mass for Case A with R11

ACQUISITION LOOP			
Cooling Load	Q_{cool}	100	kW
Cooling Temperature	T_{cool}	275	K

HEAT PUMP			
Temperature Drop HX$_{in}$	ΔT_{HXin}	5	K
Temperature Drop HX$_{out}$	ΔT_{HXout}	5	K
Input Temperature	T_{low}	270	K
Output Temperature	T_{high}	365	K
Heat Pump Efficiency	COP	1.06	
Compressor Power	W	94.0	kW
Rejection Heat Load	Q_{reject}	194.0	kW
Evaporator Spec. Mass	m_{evap}	2.72	kg/kW
Condenser/HX Spec. Mass	m_{cond}	2.72	kg/kW
Compressor Spec. Mass	m_{comp}	0.202	kg/kW
Evaporator Mass	M_{evap}	272	kg
Condenser/HX Mass	M_{cond}	527.8	kg
Compressor Mass	M_{comp}	19.0	kg
Heat Pump Mass	M_{HP}	818.8	kg

POWER SUPPLY			
Power Supply Spec. Mass	m_{power}	30	kg/kW
Power Penalty	M_{power}	2821.4	kg

REJECTION LOOP			
Liquid Pipe Mass	M_{liquid}	213.3	kg
Vapor Pipe Mass	M_{vapor}	117.5	kg
Pipe Mass	M_{pipe}	330.8	kg

RADIATOR			
Rejection Temperature	T_{reject}	360	K
Sink Temperature	T_{sink}	320	K
Fin Efficiency	η	0.7	
Emissivity	ϵ	0.8	
Radiator Area	A	968.5	m^2
Radiator Spec. Mass	m_{rad}	2.5	kg/m^2
Radiator Mass	M_{rad}	2421.3	kg

SYSTEM			
System Mass	M_{TCS}	6392	kg

Table 4: Optimum Component and TCS Mass for Case B with R717

ACQUISITION LOOP			
Cooling Load	Q_{cool}	100	kW
Cooling Temperature	T_{cool}	275	K

HEAT PUMP			
Temperature Drop HX$_{in}$	ΔT_{HXin}	5	K
Temperature Drop HX$_{out}$	ΔT_{HXout}	5	K
Input Temperature	T_{low}	270	K
Output Temperature	T_{high}	367	K
Heat Pump Efficiency	COP	1.14	
Compressor Power	W	87.7	kW
Rejection Heat Load	Q_{reject}	187.7	kW
Evaporator Spec. Mass	m_{evap}	2.72	kg/kW
Condenser/HX Spec. Mass	m_{cond}	2.72	kg/kW
Compressor Spec. Mass	m_{comp}	0.202	kg/kW
Evaporator Mass	M_{evap}	272	kg
Condenser/HX Mass	M_{cond}	510.6	kg
Compressor Mass	M_{comp}	17.7	kg
Heat Pump Mass	M_{HP}	800.3	kg

POWER SUPPLY			
Power Supply Spec. Mass	m_{power}	30	kg/kW
Power Penalty	M_{power}	2631.3	kg

REJECTION LOOP			
Liquid Pipe Mass	M_{liquid}	193.5	kg
Vapor Pipe Mass	M_{vapor}	104.8	kg
Pipe Mass	M_{pipe}	298.3	kg

RADIATOR			
Rejection Temperature	T_{reject}	362	K
Sink Temperature	T_{sink}	320	K
Fin Efficiency	η	0.7	
Emissivity	ϵ	0.8	
Radiator Area	A	884.2	m^2
Radiator Spec. Mass	m_{rad}	2.5	kg/m^2
Radiator Mass	M_{rad}	2210.4	kg

SYSTEM			
System Mass	M_{TCS}	5940	kg

Table 5: Optimum Component and TCS Mass for Case B with R11

References

[1] Swanson, T. D., Radermacher, R., Costello, F. A., Moore, J. S., and Mengers, D. R., "Low-temperature thermal control for a lunar base", *20th Intersociety Conference on Environmental Systems*, Williamsburg, Virginia, July 9–12, 1990, Publication SP-831, pp. 39–53, SAE Paper No. 901242.

[2] Costello, F. A., and Swanson., T. D., "Lunar radiators with specular reflectors", *AIAA/ASME Thermophysics and Heat Transfer Conference*, Seattle, Washington, June 18–20, 1990, ASME Publication HTD-Vol. 135, pp. 145–150.

[3] Penswick, B., and Urieli, I., "Duplex Stirling machines", *19th Intersociety Energy Conversion Engineering Conference*, San Francisco, California, August 19–24, 1984, pp. 1823–1828, SAE Paper No. 849045.

[4] Chen, F. C., Keshock, E. G., and Murphy, R. W., "Testing of a stirling cycle cooler," *The Winter Annual Meeting of the American Society of Mechanical Engineers*, Chicago, Illinois, November 27–December 2, 1988, AES-Vol. 8, SED-Vol. 6, pp. 49–55.

[5] Cremers, C. J., Birkebak, R. C., and White, J. E., "Lunar Surface Temperatures from Apollo 12," *The Moon*, Vol. 3, No. 3, December 1971, pp. 346–351.

[6] Ewert, M. K., Petete, P. P., and Dezenitis, J., "Active thermal control systems for lunar and martian exploration," *20th Intersociety Conference on Environmental Systems*, Williamsburg, Virginia, July 9–12, 1990, Publication SP-831, pp. 55–65, SAE Paper No. 901243.

[7] Waldron, R. D., "Lunar base power requirements, options and growth," *Engineering, Construction and Operations in Space 2*, Albuquerque, New Mexico, April 22–26, 1990, Proceedings of Space 90, Part 2, pp. 1288–1297.

[8] Dexter, P. F., Watts, R. J., and Haskin, W. L., "Vapor cycle compressors for aerospace vehicle thermal management," *Aerospace Technology Conference and Exposition*, Long Beach, California, October 1–4, 1990, SAE Paper No. 901960.

[9] Reynolds, W. C., *Thermodynamic Properties in SI*, Published by the Department of Mechanical Engineering, Stanford University, Stanford, California, 1979.

[10] Meitz, H., and Gottmann, M., FORTRAN77 library to compute real gas properties, University of Arizona, Tucson, Arizona.

[11] Murray, R., AiResearch, Los Angeles, California, private communication, July 1991.

[12] Carrier Air Conditioning Company, Syracuse, New York, *System Design Manual*, 1972.

[13] Dexter, P. F., and Haskin, W. L., "Analysis of heat pump augmented systems for spacecraft thermal control," *AIAA 19th Thermophysics Conference*, Snowmass, Colorado, June 25-28, 1984, AIAA Paper No. 84-1757.

[14] Guerra, L., "A commonality assessment of lunar surface habitation," *Engineering, Construction and Operations in Space*, Albuquerque, New Mexico, August 29–31, 1988, Proceedings of Space 88, pp. 274–287.

[15] Drolen, B., "Heat pump augmented radiator for high power spacecraft thermal control," *27th Aerospace Science Meeting*, Reno, Nevada, January 9-12, 1989, Paper No. AIAA 89-0077.

[16] Landis, G. A., Bailey, S. G., Brinker, D. J., and Flood, D. J., "Photovoltaic power for a lunar base," *Acta Astronautica*, Vol. 22, 1990, pp. 197–203.

[17] Roschke, E. J., and Wen, L. C., "Preliminary system definition study for solar thermal dynamic space power systems," Technical Report D-4286, JPL, Pasadena, California, June 15, 1987.